Science of the Total Environment 624 (2018) 215–224

Contents lists available at ScienceDirect

Science of the Total Environment

journal homepage: www.elsevier.com/locate/scitotenv

Multiple approaches to assess the effects of F-53B, a Chinese PFOS alternative, on thyroid endocrine disruption at environmentally relevant concentrations

Mi Deng [a,b], Yongming Wu [b], Chao Xu [c], Yuanxiang Jin [d], Xiaoli He [e], Jinbao Wan [a,*], Xiaoling Yu [a,b], Hongmin Rao [f], Wenqing Tu [b,*]

[a] College of Environmental Resources and Chemical Engineering, Nanchang University, Nanchang 330029, China
[b] Research Institute of Poyang Lake, Jiangxi Academy of Sciences, Nanchang 330012, China
[c] College of Environment, Zhejiang University of Technology, Hangzhou 310032, China
[d] College of Biotechnology and Bioengineering, Zhejiang University of Technology, Hangzhou 310032, China
[e] College of Food Science and Technology, Nanchang University, Nanchang 330029, China
[f] Research Institute of Science and Technology Strategy, Jiangxi Academy of Sciences, Nanchang 330029, China

HIGHLIGHTS

- Thyroid endocrine disruption of F-53B was investigated combining *in vitro*, *in vivo* and *in silico* approaches.
- The levels of thyroxine (T_4) were significantly increased following F-53B exposure and depuration.
- Gene transcription modulation in the HPT axis was examined.

GRAPHICAL ABSTRACT

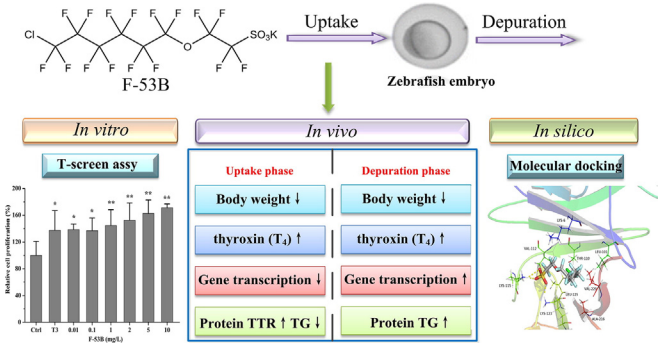

ARTICLE INFO

Article history:
Received 3 August 2017
Received in revised form 8 December 2017
Accepted 9 December 2017
Available online 15 December 2017

Editor: Kevin V. Thomas

Keywords:
F-53B
Zebrafish
Thyroid endocrine disruption
T-screen assay

ABSTRACT

A Chinese perfluorooctane sulfonate (PFOS) substitute frequently detected in the environment, 6:2 chlorinated polyfluorinated ether sulfonate (F-53B), has a similar structure to PFOS and it is proposed to cause thyroid dysfunction. To further confirm this hypothesis, the effects of F-53B on the thyroid endocrine system and underlying mechanisms were investigated *in vitro* and *in vivo* using rat pituitary GH3 cells and developing zebrafish, respectively. In GH3 cells, F-53B enhanced cell proliferation in a dose-dependent manner, indicative of thyroid receptor agonistic activity. In zebrafish larvae, F-53B exposure induced significant developmental inhibition and increased thyroxine (T_4) but not 3,5,3′-triiodothyronine (T_3) levels accompanied by a decrease in thyroglobulin (TG) protein and transcript levels of most genes involved in the hypothalamic-pituitary-thyroid (HPT) axis. Interestingly, T_4 levels remained significantly increased while TG protein and gene transcription levels were markedly upregulated after depuration. Molecular docking studies revealed that F-53B binds to transthyretin (TTR) by forming hydrogen bonds with Lys123 and Lys115, thereby interfering with thyroid hormone homeostasis. Our collective *in vitro*, *in vivo* and *in silico* studies provide novel evidence that F-53B disrupts the thyroid endocrine system at

Abbreviations: F-53B, 6:2 chlorinated polyfluorinated ether sulfonate; PFOS, perfluorooctane sulfonate; HPT axis, hypothalamic-pituitary-thyroid axis; TRs, thyroid receptors; THs, thyroid hormones; *CRH*, corticotropin-releasing hormone; *TSH*, thyroid-stimulating hormone; *DIO*, deiodinase; *TTR*, transthyretin; *NIS*, sodium/iodide symporter; *NKX2.1* (*TTF1*), thyroid transcription factor-1; *PAX8*, paired box-8; *TG*, thyroglobulin; *TPO*, thyroid peroxidase.

* Corresponding authors.
E-mail addresses: jbwan@ncu.edu.cn (J. Wan), tuwenqing@jxas.ac.cn (W. Tu).

https://doi.org/10.1016/j.scitotenv.2017.12.101
0048-9697/

environmentally relevant concentrations, which cannot be recovered after depuration. Given the persistence of F-53B in the environment, the long-term consequences of thyroid hormone disruption by this chemical warrant further investigation.

1. Introduction

In the electroplating industry, especially "hard chrome plating", perfluorooctane sulfonate (PFOS) is commonly used as an effective mist suppressant. However, due to stringent industrial regulations, a number of non-PFOS mist suppressants are beginning to appear in the market. In China, 6:2 chlorinated polyfluorinated ether sulfonate (6:2 Cl-PFAES, trade name F-53B) is widely accepted for use in the electroplating industry as a substitute for PFOS. A report by the China Metal Plating Association in 2009 revealed annual usage of 30–40 tons of mist suppressant (Lim et al., 2011). The lack of specific restrictions on emissions and disposal methods of F-53B lead to its eventual entry into the aquatic environment. Recently, F-53B was identified in surface water, wastewater and municipal sewage sludge at concentrations ranging from 2.0 to 44.2 ng/L (Lin et al., 2016), 43 to 112 μg/L (Wang et al., 2013) and 0.02 to 209 ng/L (Ruan et al., 2015), respectively. The reported contamination levels of F-53B were even higher than those of PFOS (Wang et al., 2013) and its removal by conventional wastewater treatment plants was generally below 20% (Gao et al., 2017).

Due to its similar structure to PFOS and highly lipophilicity (log *K*ow = 5.24) (Table 1), F-53B has strong bioaccumulation potential. The median log $BAF_{wholebody}$ (body bioaccumulation factors) values of F-53B in crucian carp (*Carassius carassius*) range from 4.124 to 4.322, which are higher than those of PFOS (3.430–3.279) (Shi et al., 2015). Recent studies have reported accumulation of F-53B in Greenland marine mammals (Gebbink et al., 2016) and even human serum (Pan et al., 2016). Given that F-53B is frequently detected in the environment and has high bioaccumulation capacity, sufficient attention must be paid to its potential health impacts on aquatic organisms.

Although F-53B has been used for over 30 years in the electroplating industry, knowledge about its potential toxic effects is limited. Wang et al. (2013) were the first group to report the acute toxicity of F-53B to zebrafish (LC_{50}-96 h value, 15.5 mg/L). A recent study revealed that F-53B causes developmental toxicity and disrupts cardiac development in zebrafish larvae (Shi et al., 2017). However, the mechanisms underlying these changes are yet to be established. Since thyroid hormones (TH) play a crucial role in the normal development of teleost fish, the observed adverse effects are possibly attributable to disruption of thyroid hormone homeostasis.

Our preliminary results indicate that F-53B enhances GH3 cell proliferation, confirming thyroid hormone receptors (TRs) agonistic activity. PFOS has been shown to alter TH and associated gene expression levels in zebrafish (Shi et al., 2009) and rat (Yu et al., 2009a). Based on the initial findings and structural similarities of F-53B and PFOS, the hypothesis that F-53B is a potential thyroid-disrupting chemical is plausible.

In this study, we employed rat pituitary GH3 cells and zebrafish larvae to investigate the thyroid disrupting potential of F-53B at environmentally relevant concentrations. The activity of F-53B towards TRs was evaluated in GH3 cells. In view of the unique susceptibility of developing animals to exogenous compounds and crucial roles of TH in the early stages of fish development, zebrafish larvae were employed as an *in vivo* model to examine developmental toxicity, thyroid hormone content, expression of thyroglobulin (TG) and transthyretin (TTR) proteins and transcript levels of the target genes involved in the HPT axis. Furthermore, the interaction patterns between F-53B and TTR were predicted *via* molecular docking analysis. Our results should aid in clarifying the effects of F-53B on the thyroid endocrine system that potentially lead to long-term consequences for animal and human health.

2. Materials and methods

2.1. Chemicals

F-53B (≥99% purity, CAS #73606-19-6) was obtained from Shanghai Maikun Chemical Co., Ltd. (Shanghai, China). A stock solution of F-53B was prepared in 100% dimethyl sulfoxide (DMSO) and diluted with culture medium to achieve the desired working solutions prior to the experiment. The final DMSO concentration in the control and exposure groups was 0.001% (v/v). Potassium $_L$-PFOS (≥98% purity, CAS #2795-39-3) as an internal standard was purchased from Aladdin Reagent Company (Shanghai, China). All other chemicals and solvents were of analytical grade.

2.2. CH3 cell culture and T-screen assay

The GH3 cell line was obtained from ATCC and cultured in Dulbecco's Modified Eagle's Medium/Ham's F-12 nutrient mixture supplemented with 10% fetal bovine serum (referred to as growth medium) at 37 °C in a humidified atmosphere with 5% CO_2.

Since GH3 proliferation is affected by thyroid hormone disruptors, this cell line was used for the "T-screen" assay for identifying thyroid hormone disruption compounds, which was conducted following the procedure of Kim et al. (2015) with slight modifications. Briefly, at 24 h prior to exposure, growth medium was replaced with serum-free medium to prevent cell growth due to the presence of hormones. After 24 h, cells were collected from the culture flask, plated into 96-well plates (5000 cells/well) and treated with 0, 0.01, 0.1, 1, 2, 5 or 10 mg/L F-53B. T_3 was employed as the positive control at a concentration of 1.5 μg/L. Six replicates (n = 6) were used for each treatment and control group. After a 24 h incubation period, cell proliferation was measured with the CCK-8 assay (Yeasen Biotech Company, Shanghai, China) following the manufacturer's protocol (Zou et al., 2014).

2.3. Zebrafish maintenance and experimental design

Adult wild-type zebrafish (*Danio rerio*, AB strain) maintenance and embryo exposure were performed as described previously, with slight modifications (Tu et al., 2016a). In brief, normal embryos (2 h post-

Table 1
The structure of F-53B and PFOS.

Product name	CAS no.	Formula	Molecular weight	Structure
F-53B	73606-19-6	$C_8ClF_{16}O_4SK$	570.67	
PFOS	2795-39-3	$C_8F_{17}O_3SK$	538.22	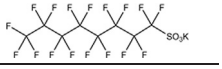

fertilization, hpf) were exposed for 5 days to 0, 0.5, 20 and 200 μg/L F-53B (equivalent to 0, 0.000875, 0.035 and 0.35 μM, respectively), followed by depuration in clean water for 5 days in 500 mL beakers. Each beaker contained 200 embryos and individual test concentrations were replicated in three beakers (n = 3), which were in the range of F-53B concentrations determined in surface water, wastewater and municipal sewage sludge (Lin et al., 2016; Ruan et al., 2015; Wang et al., 2013). F-53B-free water and water containing 0.001% DMSO were used as blank and solvent controls, respectively. Three biological replicates were used for each exposure concentration. Embryos were incubated at 28 ± 1 °C under a 14 h/10 h light/dark photoperiod. Exposure solutions were renewed daily with freshly prepared medium. At the end of uptake and depuration, 150 larvae from each replicate were randomly sampled and divided into three groups: 20 for RNA extraction, 30 for western blot analysis and 100 for TH assay. The remaining larvae were used as backup samples. Larvae were stored at −80 °C until analysis. After MS-222 anesthesia, the body lengths of individuals were measured from the forefront of the head along the body axis to the tip of the tail under an electron microscope. Zebrafish larvae after anesthesia were collected in centrifuge tubes and rinsed with ultrapure water. Excess water removed with a 10 μL pipette gun after low-speed centrifugation. The mass increase in the centrifuge tube represents the wet weight of fish. All animal procedures were carried out in accordance with the guidelines for the Care and Use of Laboratory Animals of the China Council on Animal Care and approved by the independent Animal Care Committee of Jiangxi Academy of Sciences.

2.4. Quantification of F-53B in exposure solutions

2.4.1. Sample preparation

Water samples on days 0 and 1 (T_{0d} and T_{1d}) during the uptake phase and days 1 and 5 (T_{1d} and T_{5d}) during the depuration phase were analyzed in triplicate for each treatment. Each sample was spiked with 10 ng internal standard (potassium $_L$-PFOS) and directly loaded onto an Oasis HLB cartridge (3 cm^3/60 mg, Waters, MA) at a flow rate of 1 drop/s, dried, and subsequently eluted with 2 × 0.5 mL methanol. The resulting extracts were concentrated to dryness under a gentle stream of nitrogen, dissolved in 0.5 mL of 40% methanol and filtered through a 0.22 μm nylon filter prior to analysis.

2.4.2. LC-MS/MS analysis

Quantitative analysis of F-53B was performed using an Agilent 1290 Infinity Series and Triple Quadrupole 6420 from Agilent Technology (Santa Clara, CA, USA). Chromatographic separation was performed on an Eclipase Plus C18 column (1.8 μm × 2.1 mm × 50 mm, Agilent, CA) at 35 °C using a mobile phase of 10 mM ammonium acetate in water (A) and methanol (B). The solvent gradient started at 40% B to 100% B over 3 min and was held for 1 min, followed by equilibration at 40% B for 1 min. The flow rate was 0.3 mL/min. The mass spectrometer was operated in a negative electrospray ionization mode with multiple reaction monitoring (MRM). Fragmentor voltage and collision energy were set at 160 V and 30 eV, respectively. The *m/z* 351.0 transition was selected as the quantitative product ion and sample injection volume was 5 μL. Quantification was performed *via* the internal standard approach using potassium $_L$-PFOS for F-53B.

2.5. Thyroid hormone measurements

The thyroid hormone content was measured using enzyme-linked immunosorbent assay (ELISA) based on the competitive binding enzyme immunoassay technique. Briefly, 100 larvae were sampled as one replicate (n = 3 replicates) for TH measurements. Whole-body THs were extracted as described by Kim et al. (2015). T_4 and T_3 levels were measured using commercial ELISA kits (EIAab Science Co. Ltd., Wuhan, China) according to the manufacturer's instructions. The detection limits for T_3 and T_4 were 0.1 and 1.2 ng/mL, respectively.

2.6. RNA isolation and qRT-PCR assay

Total RNA was extracted from 20 larvae (n = 3 replicates) using TRIzol reagent (Takara, Dalian, China). RNA quantification, first-strand cDNA synthesis and qRT-PCR were performed following previously described protocols (Tu et al., 2016b). Zebrafish-specific primers of the selected genes were designed using Primer 3 software (http://frodo.wi.mit.edu/). The primer sequences used in this study are listed in Supporting information (SI, Table S1). A dissociation curve was used to distinguish between the desired PCR products and primer-dimers or DNA contaminants. Prior to the analysis, we carried out a trial and confirmed the stability of *β-actin* levels under our experimental conditions. The Ct values for each gene of interest were normalized to that of *β-actin* using the $2^{-\Delta\Delta Ct}$ method (Livak and Schmittgen, 2001).

2.7. Protein extraction and western blot analysis

Western blot was performed according to our previously described procedure (Xu et al., 2016) using 30 larvae (n = 3 replicates). The detailed protocols for protein extraction are provided in SI (Text S1). Protein concentrations were determined using the BCA protein assay kit (CWBio, Beijing, China). The protein fragments were separated *via* gel electrophoresis followed by transfer to polyvinylidene difluoride membrane. The membrane was probed with primary sheep TTR, rabbit TG antibody against (Abcam, Cambridge, UK) or β-actin and further stained with horseradish peroxidase (HRP)-conjugated secondary antibodies. Sheep TTR and rabbit TG antibodies are reactive and shown to be suitable for zebrafish studies (Wang et al., 2015; Zhu et al., 2014). Bands were visualized *via* enhanced chemiluminescence and protein expression levels quantified *via* densitometry of the chemiluminescent signal. Results were normalized to β-actin expression with Quantity One v4.6 (Bio-Rad, Hercules, CA, USA).

2.8. Homology modeling and molecular docking

The three-dimensional (3D) structure of zebrafish TTR protein (zfTTR) was obtained following the homology modeling strategy (template: PDB entry 1SN0) with Modeller 9.14 (Eswar et al., 2006). Among the five models generated with Modeller 9.14, that with a GA341 score near 1.0 and low molpdf and DOPE score generally representing lower energy was selected as a favorable conformation for molecular docking. Based on the homology-modeled structure, F-53B was docked automatically into the binding site of zfTTR using AutoDock Vina 1.1.2 (http://

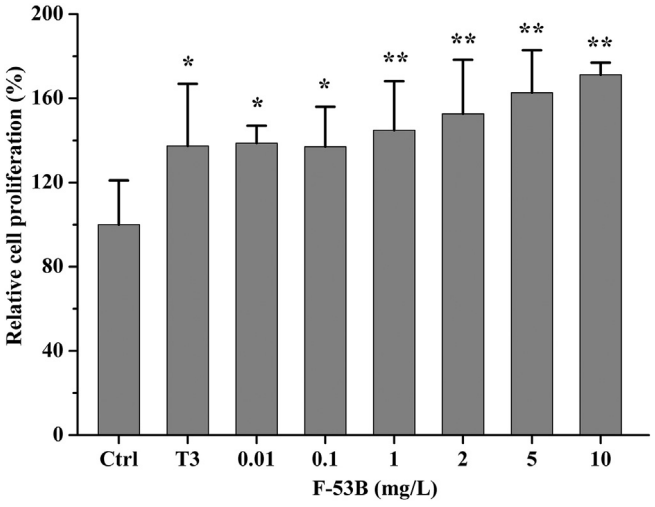

Fig. 1. Screen the effect of the F-53B towards the thyroid hormone receptor pathway using GH3 cell proliferation assay. Values represent the mean ± SD (n = 6 replicates). * indicates $p < 0.05$ and ** indicates $p < 0.01$ relative to control.

Table 2
Chemical analysis results of F-53B in the exposure solutions of replicate beakers.

Nominal concentration (μg/L)	Detected concentration (μg/L) ± SD			
	Uptake phase		Depuration phase	
	T_{0d}	T_{1d}	T_{1d}	T_{5d}
control	n.d.[a]	n.d.	n.d.	n.d.
0.5	0.26 ± 0.01	0.20 ± 0.01	n.d.	n.d.
20	12.23 ± 0.79	12.86 ± 1.08	0.82 ± 0.03	0.96 ± 0.03
200	129.15 ± 3.24	140.74 ± 4.31	6.10 ± 0.18	6.71 ± 0.33

[a] n.d. = not detected.

vina.scripps.edu/) (Trott and Olson, 2010). Detailed descriptions of homology modeling and molecular docking are provided in SI (Text S2). The superior pose with the lowest docked energy was selected and visually analyzed through application of PyMOL software (http://www.pymol.org).

2.9. Data analysis

Statistical analyses were conducted using SPSS software (Version 19.0, SPSS Inc., Chicago, IL, USA). Data are presented as means ± standard deviation (SD). The normality of data and homogeneity of variance were confirmed using the Kolmogorov-Smirnov and Levene's tests, respectively. Significant differences between the control and exposure groups were evaluated using Dunnett's one-way analysis of variance (ANOVA) with a statistical significance threshold of $p < 0.05$.

3. Results

3.1. Solvent effect

Statistical analyses revealed no significant differences in all the tested parameters between the solvent and blank control groups. Thus, data from the solvent-exposed group could be used as the control.

3.2. T-screen assay

The T-screen assay was used to characterize the thyroid hormone-disrupting effect of F-53B. As shown in Fig. 1, cell proliferation was significantly enhanced by F-53B in a dose-dependent manner. Furthermore, proliferation was evident, even in the 0.01 mg/L F-53B group, compared with the control group. Our results indicate that F-53B is a strong TH agonist.

3.3. Chemical analysis

The concentrations of F-53B in exposure solutions are shown in Table 2. F-53B was not detected in the control groups throughout the experiment. During the uptake phase, measured concentrations were 0.26, 12.23 and 129.15 μg/L in the 0.5, 20 and 200 μg/L exposure groups at T_{0d}. The rapid decrease in F-53B was mainly due to adsorption on glass surfaces (Gao et al., 2017). The concentrations at the first day before renewing (T_{1d}) were comparable with those at T_{0d}. Thus, the exposure solution was renewed daily to maintain a constant concentration. Due to the significant differences between the actual and nominal concentrations, arithmetic mean of the measured concentrations at T_{0d} and T_{1d} were used. The arithmetic mean values of exposure concentrations

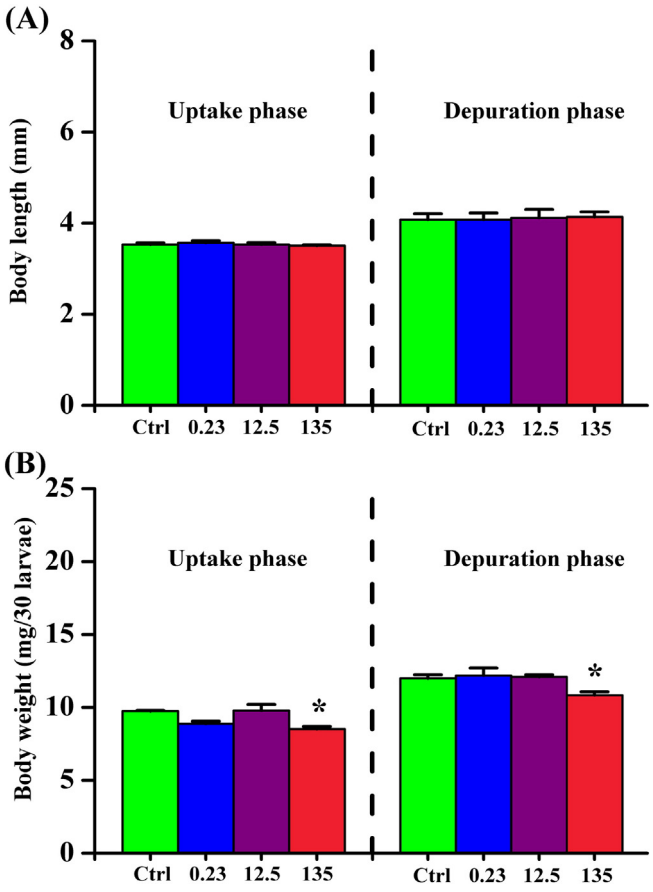

Fig. 2. The effects of F-53B on body length (A) and body weight (B) of zebrafish larvae. Values represent the mean ± SD (n = 10 replicates). * indicates $p < 0.05$ and ** indicates $p < 0.01$ relative to control.

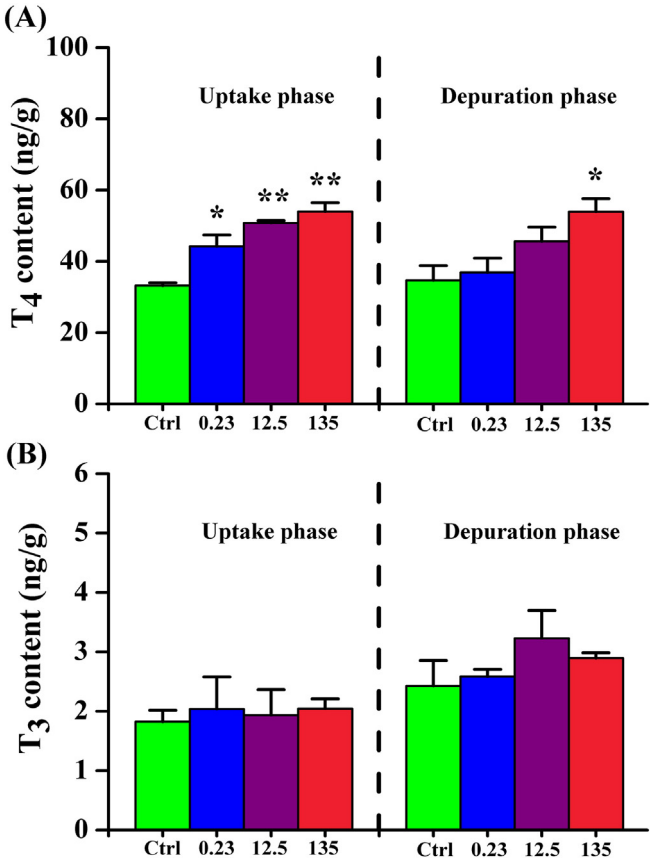

Fig. 3. The effects of F-53B on T_4 (A) and T_3 (B) levels in zebrafish larvae. Values represent the mean ± SD (n = 3 replicates). * indicates $p < 0.05$ and ** indicates $p < 0.01$ relative to control.

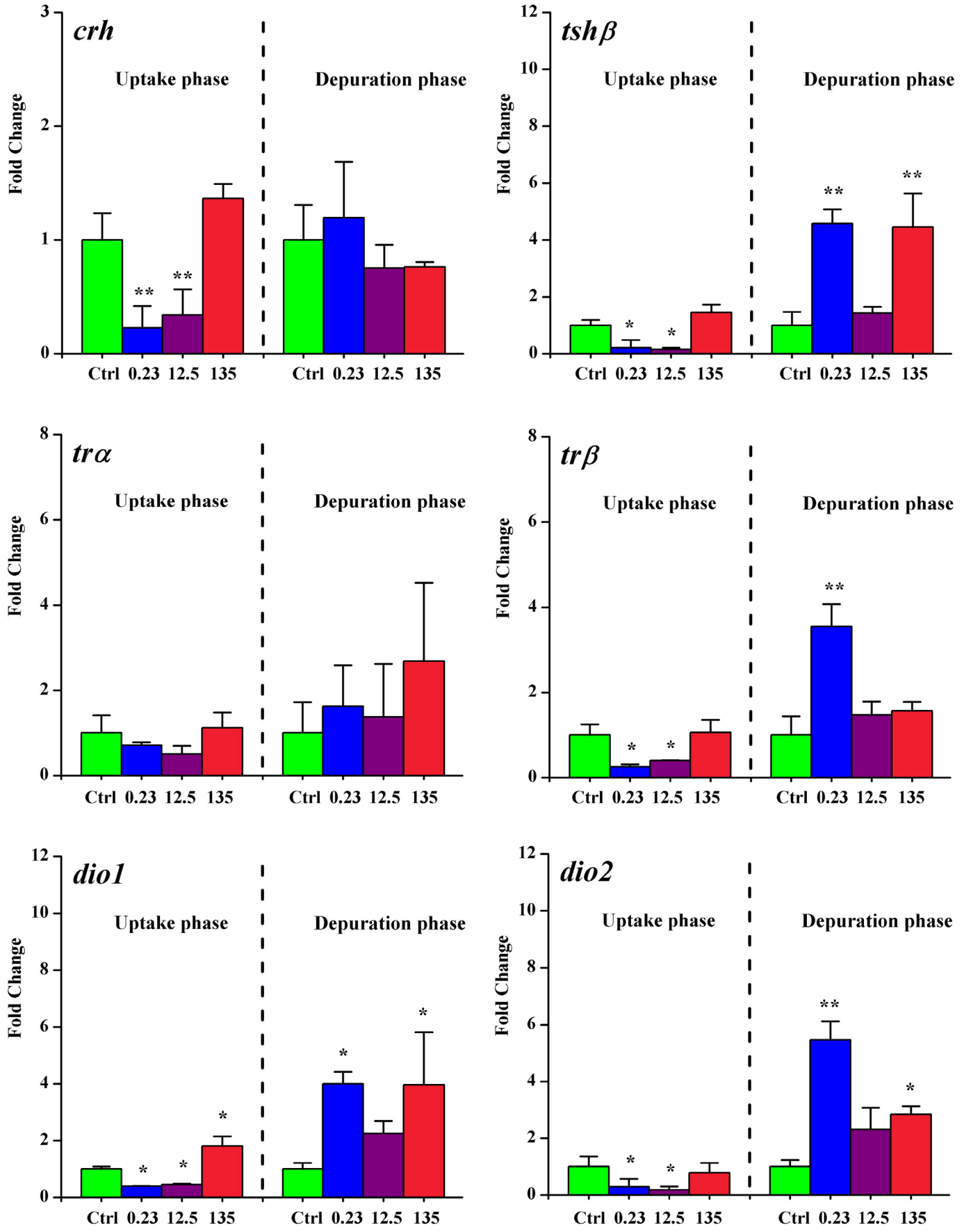

Fig. 4. The effects of F-53B on the transcription of *crh*, *tshβ*, *trα*, *trβ*, *dio1*and *dio2* genes in zebrafish larvae. Values represent the mean ± SD (n = 3 replicates). * indicates $p < 0.05$ and ** indicates $p < 0.01$ relative to control.

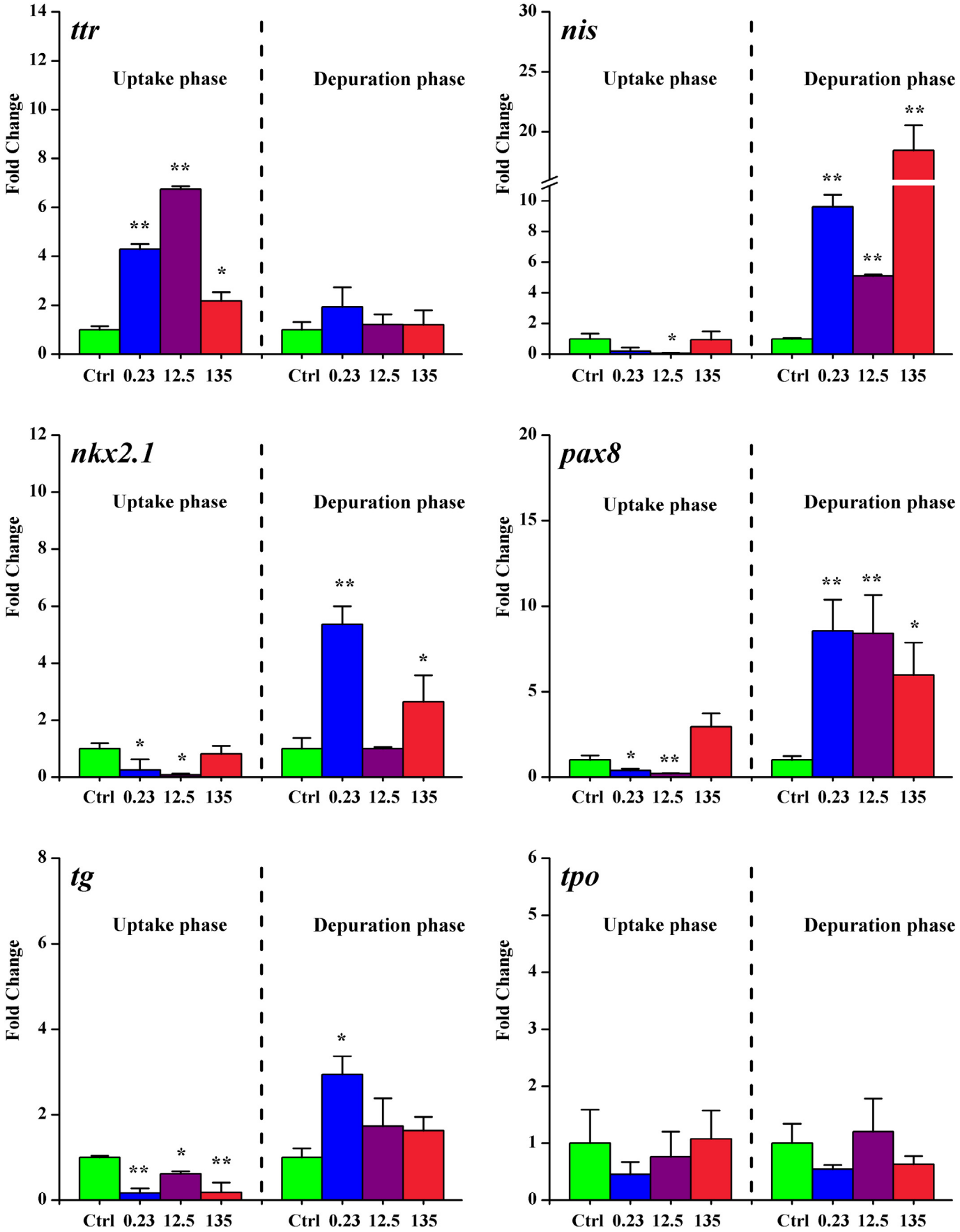

Fig. 5. The effects of F-53B on the transcription of *ttr*, *nis*, *nkx2.1*, *pax8*, *tg* and *tpo* genes in zebrafish larvae. Values represent the mean ± SD (n = 3 replicates). * indicates $p < 0.05$ and ** indicates $p < 0.01$ relative to control.

in the uptake phase were 0.23, 12.5 and 135 μg/L respectively. During the depuration phase, F-53B in the exposure solution was either not detected or present at very low levels.

3.4. Toxicological end-points

The effects of F-53B exposure and depuration on developmental toxicity of zebrafish larvae was evaluated (Fig. 2). We observed no significant effects of F-53B on body length for all groups after exposure or depuration (Fig. 2A). However, a marked decrease in body weight was observed upon treatment with 135 μg/L F-53B, which remained low after depuration, compared with the control group (Fig. 2B).

3.5. Thyroid hormone content

Exposure to F-53B resulted in a significant increase in T_4 levels in all groups (0.23–135 μg/L F-53B). After depuration, the T_4 level in the 135 μg/L F-53B treatment group remained markedly higher than that in the control group (Fig. 3A). However, there were no significant differences in T_3 levels between the treatment groups and the control group whether in the uptake or depuration phase (Fig. 3B).

3.6. Gene transcription profile

Several genes associated with regulation, transport, synthesis and metabolism of THs were examined in zebrafish larvae (Figs. 4 and 5). Following exposure to F-53B, *crh*, *tshβ*, *trβ*, *dio1*, *dio2*, *nis*, *nkx2.1* and *pax8* were significantly downregulated in the 0.23 and 12.5 μg/L treatment groups while *trα* and *tpo* levels remained unchanged. Conversely, *ttr* levels were significantly increased in all exposure groups. Expression of *tg* was markedly downregulated by 0.16-, 0.61- and 0.19-fold in the 0.23, 12.5 and 135 μg/L groups, respectively. Notably, the transcriptional levels of most genes remained unaltered, except *dio1*, upon exposure to 135 μg/L F-53B.

Depuration induced a significant increase in the transcription of *tshβ*, *trβ*, *dio1*, *dio2*, *nis*, *nkx2.1*, *pax8* and *tg* genes. In addition, expression of *crh*, *trα*, *ttr* and *tpo* was not markedly changed in all treatment groups, compared with the control group.

3.7. Expression of TTR and TG proteins

TTR and TG protein levels were assessed *via* western blot (Fig. 6). Upon treatment with 0.23, 12.5 and 135 μg/L F-53B, TTR protein was significantly upregulated by 2.9-, 3.0- and 2.1-fold, respectively. However, protein levels remained unchanged after depuration. TG protein was significantly downregulated by 0.19-fold and 0.11-fold in the 12.5 and 135 μg/L F-53B treatment groups, while levels were upregulated by 2.4-fold and 2.6-fold under the same exposure conditions after depuration, respectively.

3.8. Binding mode analysis

To clarify the potential molecular mechanism underlying the thyroid hormone- disrupting effects of F-53B, interactions between F-53B and zfTTR were explored at the molecular level. The conformation of the zfTTR/F-53B complex obtained from molecular docking studies is depicted in Fig. 7. As evident from the crystal structure of the docked zfTTR/F-53B complex, F-53B fits into the active pocket of zfTTR in the correct orientation. Further hydrogen bonding analysis revealed that F-53B forms three hydrogen bonds, one with Lys123 and two with Lys115.

4. Discussion

In the present study, levels of T_4 were significantly increased in zebrafish larvae following exposure to F-53B. This adverse effect remained unchanged after depuration, clearly indicative of a thyroid disrupting effect of F-53B at environmentally relevant concentrations. Results from the T-screen assay and molecular docking further supported the TH disrupting potential of F-53B. To our knowledge, this is the first report documenting effects of F-53B on the thyroid endocrine system.

The *in vitro* T-screen assay showed that F-53B enhances proliferation of GH3 cells in a concentration-dependent manner to a stronger extent than T_3, suggesting high thyroid hormone receptor (TR) agonistic activity. Therefore, F-53B may be considered a strong TH agonist. Additionally, the T-screen assay could be effectively applied for rapid evaluation of thyroid endocrine disruption by F-53B.

In the *in vivo* assay, T_4 levels were significantly elevated, consistent with thyroid endocrine disruption. PFOS with a chemical structure similar to F-53B is reported to disrupt the TH status in mammalian and fish models. In an earlier study, T_3 levels were significantly elevated while T_4 remained unchanged in zebrafish larvae following exposure to PFOS (Shi et al., 2009). In contrast, PFOS induced a reduction in serum T_4

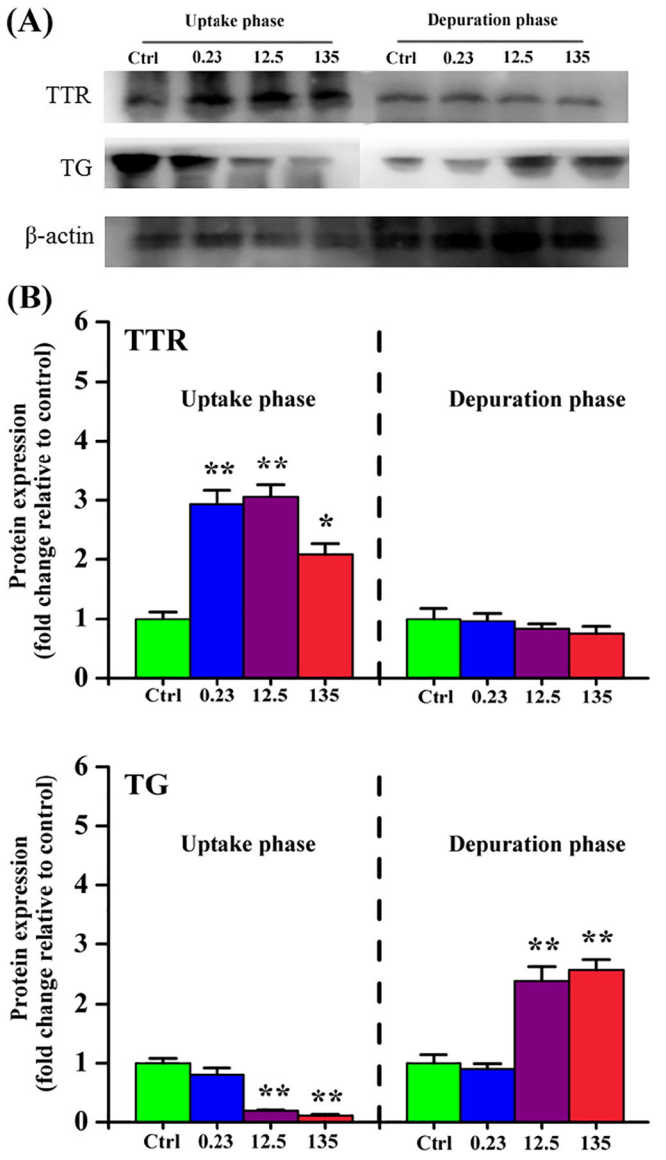

Fig. 6. The effects of F-53B on the protein expression of TTR and TG in zebrafish larvae. A representative Western blot of TTR and TG is shown in (A), with the relative quantification of TTR and TG protein expression shown in (B). Values represent the mean ± SD (n = 3 replicates). * indicates $p < 0.05$ and ** indicates $p < 0.01$ relative to control.

but did not affect T_3 levels in rat pups (Yu et al., 2009b). These reports, along with our present findings, support the theory that F-53B, as an alternative to PFOS, can similarly disrupt the thyroid endocrine system. However, the pattern of disruption may vary depending on the species, exposure dose and route. The significant decrease in body weight observed in the present study may be associated with disruption of THs, which play critical roles in fish development, especially during the early stages (Power et al., 2001). Numerous studies have reported that alterations in T_4 and T_3 levels exert adverse effects on development of fish (Tu et al., 2016a; Wang et al., 2015; Yan et al., 2012). For instance, significant inhibition of body weight and body length has been reported in association with elevated T_3 levels in zebrafish larvae after PFOS exposure (Shi et al., 2009).

The proposed interaction network of target genes involved in the HPT axis is presented in Fig. 8. In fish, *crh* stimulates the release of *tsh* from the pituitary gland, and the expression patterns of these genes are commonly used as biomarkers to determine whether thyroid dysfunction is induced by environmental chemicals (De Groef et al., 2006; Yu et al., 2011). In our study, F-53B treatment led to marked downregulation of *crh* and *tsh* (encoded by *tshβ*) genes at concentrations of 0.23 and 12.5 μg/L. In general, transcription of *crh* and *tsh* genes is modulated by alterations in TH levels through negative feedback mechanisms (Zheng et al., 2012). Upregulation of *crh* and *tshβ*, concomitant with reduction of T_4 was observed in zebrafish larvae following exposure to DE-71 (Yu et al., 2010) and microcystin-LR (Yan et al., 2012). On the other hand, PFOS increased T_3 levels accompanied by downregulation of *tshβ* in zebrafish (Shi et al., 2009). In view of these findings, we hypothesized that downregulation of *crh* and *tshβ* by F-53B may be attributable to the increase in T_4. However, mRNA levels of *crh* and *tshβ* were not significantly altered following exposure to 135 μg/L F-53B, and depuration induced an increase in *tshβ* expression. Our preliminary toxicodynamic data indicate that F-53B rapidly accumulates in zebrafish larvae and was almost not excreted from the body (SI, Table S2). Consequently, zebrafish larvae maintain high levels of internal F-53B during the depuration phase. In general, the perturbation induced by low-dose chemicals could be maintained automatically by a negative feedback mechanism, whereas at high doses this compensatory mechanism may be overwhelmed, resulting in the homeostasis to be broken (Kinoshita et al., 2006; Zhang et al., 2009). Therefore, we propose a hypothesis (as shown in Fig. 8) that at low concentrations (*i.e.* 0.23 and 12.5 μg/L) the compensatory mechanism was activated in reposes to the increased T_4 levels caused by F-53B, while at high concentrations this mechanism was overwhelmed and F-53B exerted a significant stimulating effect on the HPT axis, leading to an increase in T_4 and the upregulation of *crh* and *tshβ* genes.

TH performs its biological activity by binding to thyroid hormone receptors (TRs), including *trα* and *trβ* (Power et al., 2001). TRs are members of a large nuclear receptor superfamily that act as ligand-modulated transcription factors (Yan et al., 2012). Experiments in the present study showed downregulation of the transcript levels of *trα* and *trβ*, possibly in association with increased TH levels. Our findings were consistent with recent studies demonstrating that T_3 induced marked downregulation of *trα* and *trβ* in GH3 cells (Lee et al., 2017) and acute exposure to Tris (2-butoxyethyl) phosphate (TBOEP) led to significant increases in T_3 and T_4 accompanied by a decline in *trα* and *trβ* expression in zebrafish larvae (Liu et al., 2017). However, *trα* and *trβ* mRNA levels were upregulated after depuration, suggestive of a stimulatory effect of F-53B on TR isoforms. The observation was proposed to be attributable to prolonged exposure to high levels of internal F-53B, as discussed above.

Downregulation of *dio1* and *dio2* genes may reflect a negative feedback mechanism in response to increased T_4 levels. In fish, T_3 levels in the target organs are primarily controlled by the activities of the two deiodinases, *dio1* and *dio2*, which convert T_4 into biologically active T_3. Deiodinase activities are sensitive to environmental contaminants and their mRNA levels recommended as biomarkers for assessment of the effects of thyroid endocrine disruptors (Li et al., 2009; Shi et al., 2009). Hypothyroidism is known to enhance *dio1* and *dio2* mRNA expression and activity while hyperthyroidism suppresses these enzymes in fish (García-G et al., 2004; Orozco and Valverde-R, 2005; Van der Geyten et al., 2005). Accordingly, downregulation of *dio1* and *dio2* observed in our study is indicative of a state of hyperthyroidism. Notably, *dio1* and *dio2* were significantly upregulated after depuration. One possible explanation for this finding is failure of auto-regulation of thyroid hormone levels and a strong stimulating effect of F-53B on the HPT axis.

Significant downregulation of *nkx2.1* and *pax8* was considered part of a negative feedback mechanism associated with the increased T_4 levels. In vertebrates, transcription of several genes that stimulate synthesis of thyroid hormones, such as *nis* and *tg*, is regulated by *nkx2.1* and *pax8* in the thyroid system (Kambe et al., 1996; Zoeller et al., 2007). Therefore, the decreased transcription of *nis* and *tg* may be a result of marked downregulation of *nkx2.1* and *pax8* to counter elevation of T_4. Significant increases in *tg* and *nis* levels have been frequently reported as a potential compensatory response to decreased levels of T_4 (Chen et al., 2012; Yan et al., 2012; Yu et al., 2010). Tg is the protein precursor of TH and used for TH production by the thyroid gland. The

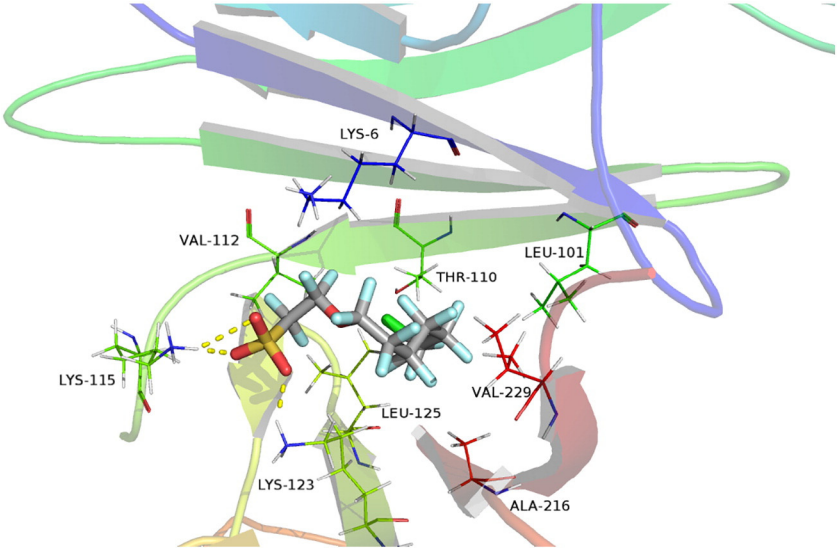

Fig. 7. Binding mode for F-53B in the binding site of zfTTR.

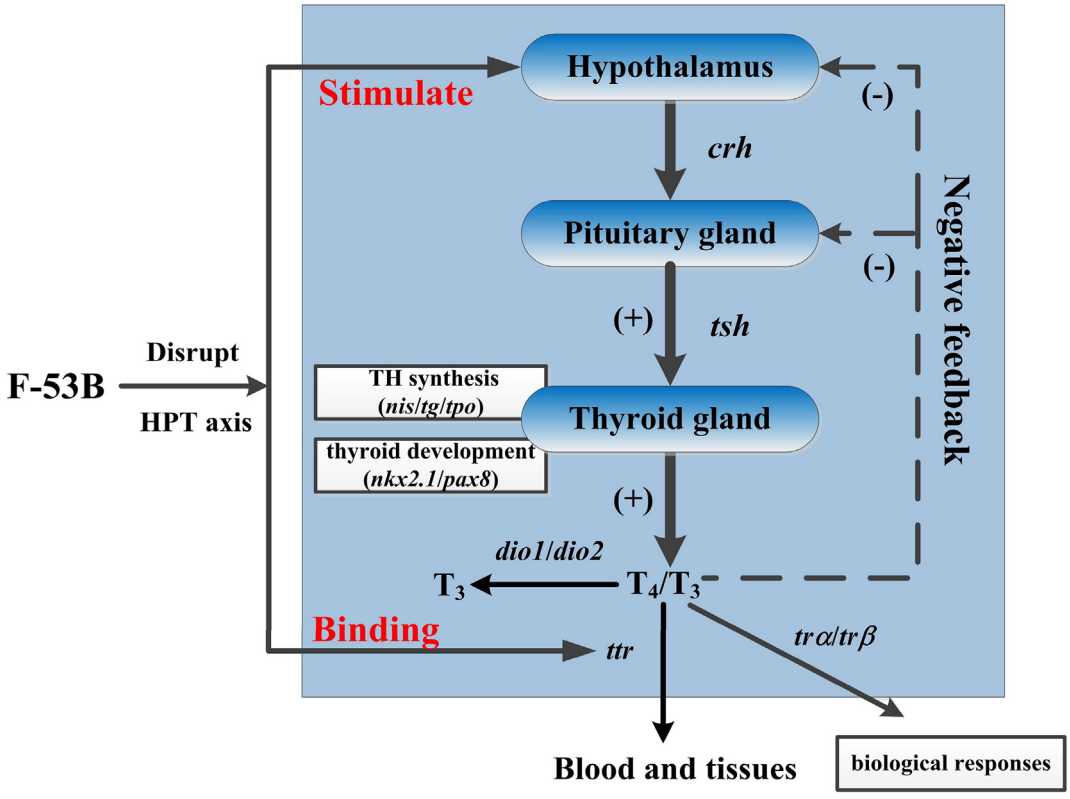

Fig. 8. Proposed interaction network of the selected genes involved in the HPT axis.

decrease in TG protein observed in this study supports the activation of a negative feedback mechanism inhibiting thyroid hormone synthesis in response to increased T_4 levels. After depuration, these genes were upregulated, potentially owing to the stimulating effect of F-53B on the HPT axis discussed above.

TTR is an important TH-binding protein in teleost fish and amphibians that interacts with and transfers THs to various target tissues (Morgado et al., 2007). The significant upregulation of *ttr* at both the transcriptional and translational levels may present a mechanism to reduce TH levels in response to elevated T_4. Our results were consistent with data from a recent study on zebrafish larvae exposed to triphenyl phosphate (Kim et al., 2015). After depuration, mRNA and protein levels of TTR were not significantly altered, indicating disruption of the negative feedback mechanism.

TTR is suggested to be one of the molecular targets of thyroid endocrine disruptors, which disturb TH homeostasis *via* competitive binding to TTR (Tu et al., 2016a; Zhang et al., 2015; Zhu et al., 2014). The observed increase in TTR mRNA and protein expression further validates the theory that TTR presents a potential target for F-53B-mediated disruption of thyroid function in zebrafish larvae. Recent years have heralded an increasing interest in the development of computational *in silico* approaches to explore the structure-toxicity relationships of toxicants. Among the multiple computational tools available, molecular docking that allows visualization of ligand-receptor interactions has been applied frequently and successfully to clarify the molecular mechanisms of action of toxicants (Cao et al., 2010; Chen et al., 2016; Li et al., 2010; Xu et al., 2016). Our molecular docking results showing that F-53B fits into the TTR ligand binding pocket and forms one hydrogen bond with Lys123 and two bonds with Lys115 further support *in vivo* outcomes. Consistent with our findings, PFOS with a similar structure to F-53B also has the ability to bind the pocket of human TTR (Kar et al., 2017; Zhang et al., 2016). Accordingly, we speculate that accumulating F-53B competes with TH to bind TTR protein, which interferes with TH homeostasis and ultimately affects the growth and development of zebrafish larvae.

In conclusion, data from the current study clearly demonstrate that F-53B triggers thyroid endocrine disruption in fish. Since the concentrations used for analysis are environmentally relevant, the thyroid hormone-disrupting effects of F-53B, often used as an alternative to PFOS, should be researched in more detail. Our results highlight the importance of combining multiple approaches (*in vitro*, *in vivo* and *in silico*) for identifying thyroid hormone disruptors that may adversely affect animal and human health and the underlying mechanisms. In view of the persistent presence of F-53B in the environment, the long-term consequences of its application warrant further investigation.

Acknowledgements

This work was supported by the National Natural Science Foundation of China (No. 21647005), Jiangxi Province Natural Science Foundation of China (No. 2016BAB213095), Key Program for Science and Technology Cooperation Projects of Jiangxi, China (20151BDH80021), Jiangxi Science and Technology Project (20133BBF60053), Key Program of Jiangxi Academy of Sciences (20161BAB213095) and Program of State Administration of Foreign Experts Affairs (P172022005).

Appendix A. Supplementary data

Supplementary data to this article can be found online at https://doi.org/10.1016/j.scitotenv.2017.12.101.

References

Cao, J., Lin, Y., Guo, L.H., Zhang, A.Q., Wei, Y., Yang, Y., 2010. Structure-based investigation on the binding interaction of hydroxylated polybrominated diphenyl ethers with thyroxine transport proteins. Toxicology 277, 20–28.

Chen, Q., Yu, L.Q., Yang, L.H., Zhou, B.S., 2012. Bioconcentration and metabolism of decabromodiphenyl ether (BDE-209) result in thyroid endocrine disruption in zebrafish larvae. Aquat. Toxicol. 110, 141–148.

Chen, Q.C., Wang, X.X., Shi, W., Yu, H.X., Zhang, X.W., Giesy, J.P., 2016. Identification of thyroid hormone disruptors among HO-PBDEs: *in vitro* investigations and coregulator involved simulations. Environ. Sci. Technol. 50, 12429–12438.

De Groef, B., Van der Geyten, S., Darras, V.M., Kuhn, E.R., 2006. Role of corticotropin-releasing hormone as a thyrotropin-releasing factor in non-mammalian vertebrates. Gen. Comp. Endocrinol. 146, 62–68.

Eswar, N., Webb, B., Marti-Renom, M.A., Madhusudhan, M., Eramian, D., Shen, M.y., Pieper, U., Sali, A., 2006. Comparative protein structure modeling using Modeller. Curr. Protoc. Bioinformatics 86, 5.6.1–5.6.30.

Gao, Y., Deng, S., Du, Z., Liu, K., Yu, G., 2017. Adsorptive removal of emerging polyfluoroalky substances F-53B and PFOS by anion-exchange resin: a comparative study. J. Hazard. Mater. 323, 550–557.

Garćia-G, C., Jeziorski, M.C., Valverde-R, C., Orozco, A., 2004. Effects of iodothyronines on the hepatic outer-ring deiodinating pathway in killifish. Gen. Comp. Endocr. 135 (2), 201–209.

Gebbink, W.A., Bossi, R., Rigét, F.F., Rosing-Asvid, A., Sonne, C., Dietz, R., 2016. Observation of emerging per-and polyfluoroalkyl substances (PFASs) in Greenland marine mammals. Chemosphere 144, 2384–2391.

Kambe, F., Nomura, Y., Okamoto, T., Seo, H., 1996. Redox regulation of thyroid-transcription factors, Pax-8 and TTF-1, is involved in their increased DNA-binding activities by thyrotropin in rat thyroid FRTL-5 cells. Mol. Endocrinol. 10, 801–812.

Kar, S., Sepúlveda, M.S., Roy, K., Leszczynski, J., 2017. Endocrine-disrupting activity of per- and polyfluoroalkyl substances: exploring combined approaches of ligand and structure based modeling. Chemosphere 184, 514–523.

Kim, S., Jung, J., Lee, I., Jung, D., Youn, H., Choi, K., 2015. Thyroid disruption by triphenyl phosphate, an organophosphate flame retardant, in zebrafish (*Danio rerio*) embryos/larvae, and in GH3 and FRTL-5 cell lines. Aquat. Toxicol. 160, 188–196.

Kinoshita, A., Wanibuchi, H., Wei, M., Fukushima, S., 2006. Hormesis in carcinogenicity of non-genotoxic carcinogens. J. Toxicol. Pathol. 19 (3), 111–122.

Lee, S., Kim, C., Youn, H., Choi, K., 2017. Thyroid hormone disrupting potentials of bisphenol A and its analogues-*in vitro* comparison study employing rat pituitary (GH3) and thyroid follicular (FRTL-5) cells. Toxicol. in Vitro 40, 297–304.

Li, W., Zha, J.M., Spear, P.A., Li, Z.L., Yang, L.H., Wang, Z.J., 2009. Changes of thyroid hormone levels and related gene expression in Chinese rare minnow (*Gobiocypris rarus*) during 3-amino-1,2,4-triazole exposure and recovery. Aquat. Toxicol. 92, 50–57.

Li, F., Xie, Q., Li, X.H., Li, N., Chi, P., Chen, J.W., Wang, Z.J., Hao, C., 2010. Hormone activity of hydroxylated polybrominated diphenyl ethers on human thyroid receptor-β: in vitro and in silico investigations. Environ. Health Perspect. 118, 602.

Lim, T.C., Wang, B., Huang, J., Deng, S., Yu, G., 2011. Emission inventory for PFOS in China: review of past methodologies and suggestions. Sci. World J. 11, 1963–1980.

Lin, Y., Liu, R., Hu, F., Liu, R., Ruan, T., Jiang, G., 2016. Simultaneous qualitative and quantitative analysis of fluoroalkyl sulfonates in riverine water by liquid chromatography coupled with Orbitrap high resolution mass spectrometry. J. Chromatogr. A 1435, 66–74.

Liu, Y.R., Wu, D., Xu, Q.L., Yu, L.Q., Liu, C.S., Wang, J.H., 2017. Acute exposure to tris (2-butoxyethyl) phosphate (TBOEP) affects growth and development of embryo-larval zebrafish. Aquat. Toxicol. 191, 17–24.

Livak, K.J., Schmittgen, T.D., 2001. Analysis of relative gene expression data using real-time quantitative PCR and the 2(T)(−Delta Delta C) method. Methods 25, 402–408.

Morgado, I., Santos, C.R.A., Jacinto, R., Power, D.M., 2007. Regulation of transthyretin by thyroid hormones in fish. Gen. Comp. Endocrinol. 152, 189–197.

Orozco, A., Valverde-R, C., 2005. Thyroid hormone deiodination in fish. Thyroid 15, 799–813.

Pan, Y., Zhu, Y., Zheng, T., Cui, Q., Buka, S.L., Zhang, B., Guo, Y., Xia, W., Yeung, L.W., Li, Y., 2016. Novel chlorinated polyfluorinated ether sulfonates and legacy per-/polyfluoroalkyl substances: placental transfer and relationship with serum albumin and glomerular filtration rate. Environ. Sci. Technol. 51, 634–644.

Power, D.M., Llewellyn, L., Faustino, M., Nowell, M.A., Bjornsson, B.T., Einarsdottir, I.E., Canario, A.V.M., Sweeney, G.E., 2001. Thyroid hormones in growth and development of fish. Comp. Biochem. Physiol., Part C: Toxicol. Pharmacol. 130, 447–459.

Ruan, T., Lin, Y., Wang, T., Liu, R., Jiang, G., 2015. Identification of novel polyfluorinated ether sulfonates as PFOS alternatives in municipal sewage sludge in China. Environ. Sci. Technol. 49, 6519–6527.

Shi, X.J., Liu, C.S., Wu, G.Q., Zhou, B.S., 2009. Waterborne exposure to PFOS causes disruption of the hypothalamus-pituitary-thyroid axis in zebrafish larvae. Chemosphere 77, 1010–1018.

Shi, Y., Vestergren, R., Zhou, Z., Song, X., Xu, L., Liang, Y., Cai, Y., 2015. Tissue distribution and whole body burden of the chlorinated polyfluoroalkyl ether sulfonic acid F-53B in crucian carp (*Carassius carassius*): evidence for a highly bioaccumulative contaminant of emerging concern. Environ. Sci. Technol. 49, 14156–14165.

Shi, G.H., Cui, Q.Q., Pan, Y.T., Sheng, N., Sun, S.J., Guo, Y., Dai, J.Y., 2017. 6:2 chlorinated polyfluorinated ether sulfonate, a PFOS alternative, induces embryotoxicity and disrupts cardiac development in zebrafish embryos. Aquat. Toxicol. 185, 67–75.

Trott, O., Olson, A.J., 2010. Software news and update AutoDock Vina: improving the speed and accuracy of docking with a new scoring function, eficient optimization, and multithreading. J. Comput. Chem. 31, 455–461.

Tu, W.Q., Xu, C., Jin, Y.X., Lu, B., Lin, C.M., Wu, Y.M., Liu, W.P., 2016a. Permethrin is a potential thyroid-disrupting chemical: *in vivo* and *in silico* envidence. Aquat. Toxicol. 175, 39–46.

Tu, W.Q., Xu, C., Lu, B., Lin, C.M., Wu, Y.M., Liu, W.P., 2016b. Acute exposure to synthetic pyrethroids causes bioconcentration and disruption of the hypothalamus–pituitary–thyroid axis in zebrafish embryos. Sci. Total Environ. 542, 876–885.

Van der Geyten, S., Byamungu, N., Reyns, G., Kuhn, E., Darras, V., 2005. Iodothyronine deiodinases and the control of plasma and tissue thyroid hormone levels in hyperthyroid tilapia (*Oreochromis niloticus*). J. Endocrinol. 184, 467–479.

Wang, S., Huang, J., Yang, Y., Hui, Y., Ge, Y., Larssen, T., Yu, G., Deng, S., Wang, B., Harman, C., 2013. First report of a Chinese PFOS alternative overlooked for 30 years: its toxicity, persistence, and presence in the environment. Environ. Sci. Technol. 47, 10163–10170.

Wang, Q.W., Lai, N.L.-S., Wang, X.F., Guo, Y.Y., Lam, P.K.-S., Lam, J.C.-W., Zhou, B.S., 2015. Bioconcentration and transfer of the organophorous flame retardant 1, 3-dichloro-2-propyl phosphate causes thyroid endocrine disruption and developmental neurotoxicity in zebrafish larvae. Environ. Sci. Technol. 49, 5123–5132.

Xu, C., Tu, W.Q., Deng, M., Jin, Y.X., Lu, B., Zhang, C.N., Lin, C.M.A., Wu, Y.M., Liu, W.P., 2016. Stereoselective induction of developmental toxicity and immunotoxicity by acetochlor in the early life stage of zebrafish. Chemosphere 164, 618–626.

Yan, W., Zhou, Y.X., Yang, J., Li, S.Q., Hu, D.J., Wang, J.H., Chen, J., Li, G.Y., 2012. Waterborne exposure to microcystin-LR alters thyroid hormone levels and gene transcription in the hypothalamic-pituitary-thyroid axis in zebrafish larvae. Chemosphere 87, 1301–1307.

Yu, W.G., Liu, W., Jin, Y.H., 2009a. Effects of perfluorooctane sulfonate on rat yhyroid hormone biosynthesis and metabolism. Environ. Toxicol. Chem. 28, 990–996.

Yu, W.G., Liu, W., Jin, Y.H., Liu, X.H., Wang, F.Q., Liu, L., Nakayama, S.F., 2009b. Prenatal and postnatal impact of perfluorooctane sulfonate (PFOS) on rat development: a cross-foster study on chemical burden and thyroid hormone system. Environ. Sci. Technol. 43, 8416–8422.

Yu, L.Q., Deng, J., Shi, X.J., Liu, C.S., Yu, K., Zhou, B.S., 2010. Exposure to DE-71 alters thyroid hormone levels and gene transcription in the hypothalamic-pituitary-thyroid axis of zebrafish larvae. Aquat. Toxicol. 97, 226–233.

Yu, L.Q., Lam, J.C., Guo, Y.Y., Wu, R.S., Lam, P.K., Zhou, B.S., 2011. Parental transfer of polybrominated diphenyl ethers (PBDEs) and thyroid endocrine disruption in zebrafish. Environ. Sci. Technol. 45, 10652–10659.

Zhang, Q., Pi, J.B., Woods, C.G., Andersen, M.E., 2009. Phase I to II cross-induction of xenobiotic metabolizing enzymes: a feedforward control mechanism for potential hormetic responses. Toxicol. Appl. Pharmacol. 237 (3), 345–356.

Zhang, J., Kamstra, J.H., Ghorbanzadeh, M., Weiss, J.M., Hamers, T., Andersson, P.L., 2015. *In silico* approach to identify potential thyroid hormone disruptors among currently known dust contaminants and their metabolites. Environ. Sci. Technol. 49, 10099–10107.

Zhang, J., Begum, A., Brännström, K., Grundström, C., Iakovleva, I., Olofsson, A., Sauer-Eriksson, A.E., Andersson, P.L., 2016. Structure-based virtual screening protocol for in silico identification of potential thyroid disrupting chemicals targeting transthyretin. Environ. Sci. Technol. 50 (21), 11984–11993.

Zheng, X.M., Zhu, Y.T., Liu, C.S., Liu, H.L., Giesy, J.P., Hecker, M., Lam, M.H.W., Yu, H.X., 2012. Accumulation and biotransformation of BDE-47 by zebrafish larvae and teratogenicity and expression of genes along the hypothalamus-pituitary-thyroid axis. Environ. Sci. Technol. 46, 12943–12951.

Zhu, B.R., Wang, Q.W., Wang, X.F., Zhou, B.S., 2014. Impact of co-exposure with lead and decabromodiphenyl ether (BDE-209) on thyroid function in zebrafish larvae. Aquat. Toxicol. 157, 186–195.

Zoeller, R.T., Tan, S.W., Tyl, R.W., 2007. General background on the hypothalamic-pituitary-thyroid (HPT) axis. Crit. Rev. Toxicol. 37, 11–53.

Zou, X.Y., Shi, J.P., Zhang, H.W., 2014. Coexistence of silver and titanium dioxide nanoparticles: enhancing or reducing environmental risks? Aquat. Toxicol. 154, 168–175.